Clinical Neurophysiology 122 (2011) 1440–1447

Contents lists available at ScienceDirect

Clinical Neurophysiology

journal homepage: www.elsevier.com/locate/clinph

Somatosensory-evoked potentials as an indicator for the extent of ultrastructural damage of the spinal cord after chronic compressive injuries in a rat model

Yong Hu [a,*,1], Chun-Yi Wen [a,1], Ting-Hung Li [a], Matthew Man-Hin Cheung [b], Ed Xue-kui Wu [b], Keith Dip-Kei Luk [a]

[a] Department of Orthopaedics and Traumatology, Li Kai Shing Faculty of Medicine, The University of Hong Kong, Hong Kong, PR China
[b] Department of Electrical and Electronic Engineering, The University of Hong Kong, Hong Kong, PR China

ARTICLE INFO

Article history:
Accepted 17 December 2010
Available online 16 February 2011

Keywords:
Spinal cord
Chronic compression
Ultrastructure
Magnetic resonance imaging (MRI)
Micro-computed tomography (μCT)

HIGHLIGHTS

- Spatial filter based on Probabilistic Independent component analysis (PICA) to isolate Somatosensory-evoked potentials (SEP) related components and enhance the signal-to-noise-ratio (SNR) of event related potentials (ERPs).
- Time-frequency filter based on continuous Wavelet filtering to significantly enhance the SNR of ERPs.
- Combining PICA and wavelet filtering offers a space-time-frequency filter to provide a reliable estimation of single-trial ERPs.

ABSTRACT

Objective: Somatosensory-evoked potentials (SEPs) were found to correlate well with the disability and postoperative recovery in patients with cervical spondylotic myelopathy. Yet the exact pathophysiology behind it remains to be elucidated. This study aims to characterise the ultrastructural changes of a chronically compressive spinal cord with various SEP responses in a rat model.
Methods: A total of 15 rats were used with surgical implantation of a water-absorbing polymer sheet into the cervical spinal canal on the postero–lateral side, which expanded over time to induce chronic compression in the cord. At postoperative 6 months, the functional integrity of the cords was recorded by SEP responses by comparing injured and non-injured sides, and the ultrastructural integrity was assessed by 7-T magnetic resonance (MR) diffusion imaging, contrast-enhanced micro-computed tomography (μCT) and histological evaluations.
Results: Six rats showed unchanged SEP, and the other nine showed decreased amplitude only ($n = 5$) or delayed latency ($n = 4$). The circulation insults of the cords were found among all the rats, showing central canal enlargement, intra-tissue bleeding or increased blood vessels in the central grey matter. Ultrastructural damage was noted in the rats with changed SEP responses, which was suggested by lower fractional anisotropy and higher contrast intensity radiologically and echoed by less myelin stain and cavitation changes histologically. In the animals with delayed latency, the cord showed significant loss of motoneurons as well as gross appearance distortion.
Conclusions: The categorised SEP responses by amplitude and latency could be an indicator for the extent of ultrastructural damage of the spinal cord after chronic compressive injuries.
Significance: The findings built a solid foundation for SEP application in clinical diagnosis and prognostication of spinal cord injuries.

1. Introduction

Cervical spondylotic myelopathy (CSM) is the most common type of spinal cord dysfunction in patients older than 55 years (Rao, 2002; Ichihara et al., 2003; McCormick et al., 2003). It is caused by spinal stenosis, that is, spondylosis, disc degeneration and ossification of the posterior longitudinal ligament, etc., with

* Corresponding author. Address: Department of Orthopeadics and Traumatology, The University of Hong Kong, 12 Sandy Bay Road, Pokfulam, Hong Kong, PR China. Tel.: +852 29740359; fax: +852 29740335.
E-mail address: yhud@hkusua.hku.hk (Y. Hu).
[1] Authors who contributed equally to this work.

1388-2457/$36.00
doi:10.1016/j.clinph.2010.12.051

induced chronic compression on the cord and the subsequent motor and sensory functional deficit. However, the insidious onset of CSM, the variety of clinical signs and symptoms and lack of objective evaluation tool pose a big challenge to make an early diagnosis and precise prognostication for surgical decompression (McCormick et al., 2003; Baron and Young, 2007).

Somatosensory-evoked potentials (SEPs), which were commonly used for intra-operative monitoring of the spinal cord (Hu et al., 2003), has been introduced for the diagnosis and prognostication of CSM (Lo, 2007, 2008). Apart from the monitoring value, SEPs can provide information of prognostic relevance because they directly assess the physiological integrity of the spinal cord (Robinson et al., 2003). Preoperative SEP testing together with clinical signs can predict preclinical spondylotic cervical cord compression (Bednarik et al., 2004). A previous study showed that intra-operative SEP responses can predict short-term postoperative clinical improvement. Normal or slightly abnormal SEPs, for example, may suggest an incomplete lesion and then indicate a better prognosis for recovery (Morishita et al., 2005). However, SEP responses were classified as normal and abnormal types; it cannot predict long-term prognosis, which decreased the prognostic value of SEP (Bouchard et al., 1996). In our previous study, the SEP responses were further categorised based on the latency and amplitude, instead of simply being described as normal or abnormal SEP responses. It was found that the categorised SEP responses by the latency and amplitude correlated well with the CSM patients' symptoms and postoperative recovery (Hu et al., 2008). It was reported that there was over 50% improvement in the symptoms in patients with normal SEP responses or decreased amplitude only; in contrast, the recovery in those with prolonged latency or loss of SEP response was poor with only 20–30% improvement. It might suggest the potential value of SEP responses as the indicator for the severity of ultrastructural damage of the spinal cord after chronic compressive injury. Yet, the exact pathophysiology behind the normal and abnormal SEP responses has rarely been studied in chronic spinal cord injuries.

The present study was designed to: (1) develop a model of spinal cord chronic compressive injuries in rat to mimic the natural course of CSM and (2) group the animals based on the categorised SEP responses by the latency and amplitude, and then compare the ultrastructural characteristics of the spinal cords among them. Multiple advanced bioimaging modalities, including 7-T magnetic resonance imaging (MRI) and contrast-enhanced micro-computed tomography (μCT), were applied for evaluation of ultrastructural changes of the spinal cords after chronic compression as well as routine histological evaluation.

2. Materials and methods

2.1. Study design

A total of 15 female adult Sprague–Dawley (SD) rats (250–300 g) were used in this study. All experimental procedures were approved by the Research Ethics Committee of the authors' institutes. The animals were operated with implantation of a water-absorbing polymer sheet into the cervical spinal canal, which expanded over time to induce chronic compression to the cord. At postoperative 6 months, the functional integrity of the cord was evaluated by the SEPs. The ultrastructure of the cord was evaluated by advanced bioimaging modalities, that is, 7-T MRI and contrast-enhanced μCT and routine histology.

2.2. Induction of spinal cord chronic compression

The animals were operated under microscopy by a trained spine surgeon according to an established surgical protocol for implantation of water-absorbing materials (Kim et al., 2004). In brief, the animals were operated under general anaesthesia with 10% ketamine/2% xylazine (Kethalar, 1 ml: 1 ml) intraperitoneally (Sigma Chemical Co., St. Louis, MO, USA). After the occipital and nuchal areas were shaved and prepared with iodine solution, a skin incision was made to expose the laminae C3–C7 on one side with removal of ligamentum flavum between them through a posterior approach under microscopy. A small space around the facet was opened with laminotomy and enlarged with natural flexion of the spine. The dura underneath was carefully separated from the laminae to prevent leakage of cerebrospinal fluid. SEP was monitored to exclude any spinal cord injury induced during the surgical operation. A thin sheet polymer, (14)-3,6-anhydro-α-L-galactopyranosyl-(13)-β-D-galactopyranan, was then carefully inserted into the lateral side of rat spinal canal at C5 level (Fig. 1). The polymer was coated with a sustained-release membrane to control interstitial fluid absorption from the surrounding tissues and reach maximum expansion in 24 h and remain at the maximal volume for 6 months. Thereafter, it could produce a chronic course of compression on the cervical spinal cord in rat. After implantation, the incision site was closed by layers and the animals were allowed back to the cage until fully recovering from the surgery on a heating bed.

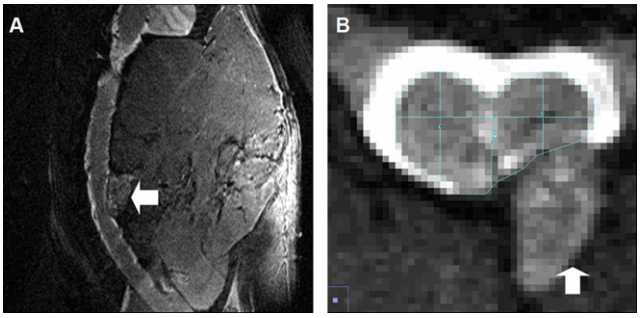

Fig. 1. The representative saggittal (A) and axial (B) magnetic resonance images of rat spinal cord with the surgically implanted polymers (white matter). The polymer, with the formula (14)-3, 6-anhydro-α-L-galactopyranosyl-(13)-D-galactopyranan, was surgically implanted into the spinal canal at the C5 level from the postero–lateral side after removal of lamina at C3–C7 levels of the cord in model rats. A small space around facet was opened with laminotomy and enlarged with natural flexion of the spine.

2.3. Electrophysiological evaluations

Functional integrity of the cord among the model rats were evaluated by SEPs using our established protocol (Zhang et al., 2009). The animals were evaluated under general anaesthesia with 10% ketamine/2% xylazine (Kethalar, 1 ml: 1 ml) intraperitoneally (Sigma Chemical Co., St. Louis, MO, USA). To elicit cortical SEP, a constant current stimulator was used with a 5.1 Hz square wave 0.2 ms in duration to stimulate the tibial nerve along the course of the gastrocnemius muscle belly. The stimulation intensity was selected as twice the motor threshold. The motor threshold can be established by increasing the intensity gradually until a twitch in the gastrocnemius muscle is seen. During the SEP test, the effectiveness of nerve stimulation was evaluated by visual inspection on the twitch in the appropriate innervated muscle group, which ensured that adequate stimulation was applied. The cortical SEP was recorded from the skull at Cz–Fz. The signal was amplified 100,000 times with two amplifiers (SCXI-1120, National Instruments Co., TX, USA). Band-pass filtering between 2 and 2000 Hz was used. All the SEP signals were acquired with a data acquisition card (DAQcard-1200, National Instruments Co., TX, USA) at 12-bit

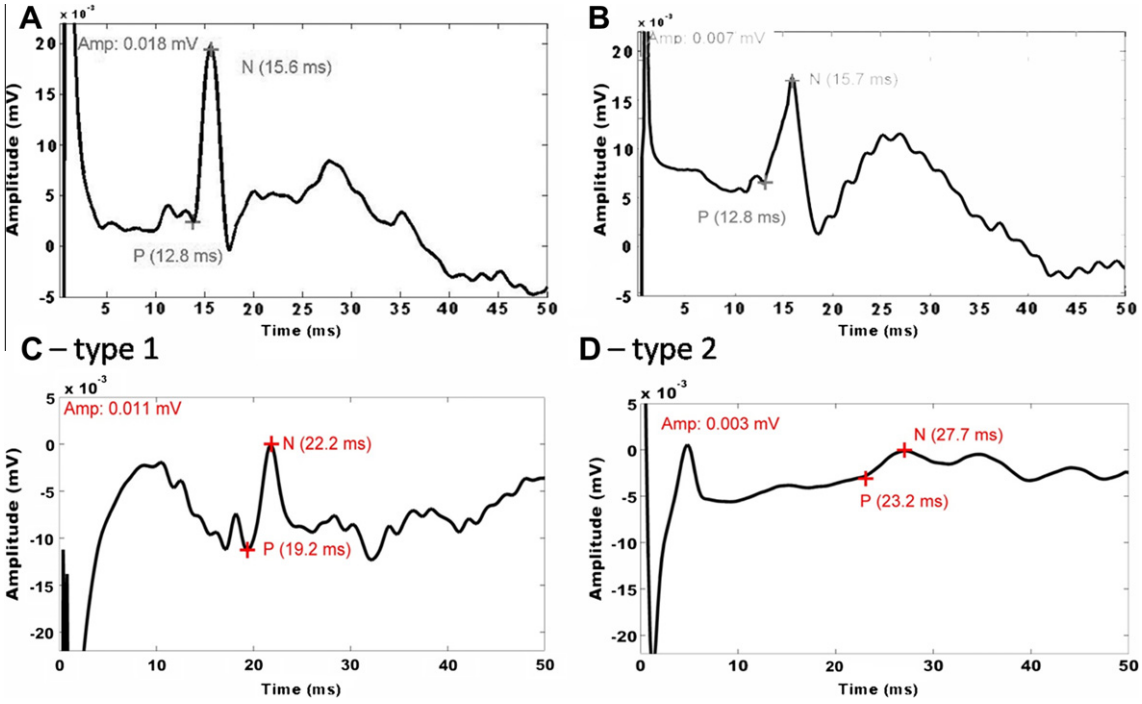

Fig. 2. The samples of the categories of the somatosensory-evoked potentials (SEP) responses in model rats. The onset latency was measured by the time delay of P while the amplitude was measured by the voltage differences between P and N. Based on the injured and non-injured sides difference of onset latency and amplitude of the SEP responses to the stimulations, the animals were grouped as: I: normal latency and amplitude (group A); II: normal latency and abnormal amplitude (group B); III: abnormal latency and either normal (Group C: type 1) or abnormal amplitude (Group C: type 2).

resolution and a sampling rate of 5000 Hz. To obtain a good quality of the SEP signals, a total of 500 SEP responses were averaged for each trial. All the following signal processing programmes were developed in the MATLAB environment (version 7.0, Mathworks, MA, USA) using a Pentium 4 PC platform (3.2 GHz, 1 Gbytes RAM). The SEP response was identified and the latency delay and amplitude of the response were then determined (Fig. 2). Based on the difference in the injured and non-injured sides in terms of onset latency and amplitude of SEP responses to the stimulations, the model rats were grouped into three types: (A) unchanged (normal) latency and amplitude; (B) normal latency and abnormal amplitude; (C) abnormal latency with either normal or abnormal amplitude.

2.4. Magnetic resonance imaging evaluations

The cord compression was evaluated under magnetic resonance imaging (MRI) using our established protocol (Cheung et al., 2009). The animals were anaesthetised with the inhalation of isoflurane and a surface coil was placed over the cervical spine region; anatomical T2-weighted (T2W) and proton density weighted (PDW) images were acquired with a 7T Bruker PharmaScan 70/16 scanner (Bruker, Germany). T2W and PDW images were acquired with the parameters as followed: Time of echo (TE)/Time of repetition (TR) = 35/2500 ms (T2W) and 115/2500 ms (PDW), slice thickness = 1 mm, interslice distance = 1.1 mm, number of excitation (NEX) = 4. A total of 15 axial slices covering C3–C7 of the cervical spinal cord were acquired at each disc and body levels. Diffusion tensor imaging (DTI) was acquired using multi-shot spin-echo echo-planar imaging (SE-EPI), with navigator echo in 30 diffusion directions. The imaging parameters were as follows: *b*-value = 600 s mm^{-2}, slice thickness = 7 mm, TE/TR = 29/3000 ms, slice gap = 2.2 mm, pixel size = 0.234 × 0.234 × 2.0 mm^3 and NEX4. The image slice planning was the same as that in anatomical axial images, with 15 slices covering the cervical spinal cord from C3 to C7. DTI data analysis was performed with the software DTI Studio (version 2.4.01, 2003, John Hopkins Medical Institute, John Hopkins University, Baltimore, MD, USA). After imaging co-registration, fractional anisotropy (FA) maps were generated and the values were calculated in white matter on the injured and non-injured sides, respectively.

2.5. Micro-computed tomography evaluations

Thereafter, the rats were sacrificed and treated by perfusion of paraformaldehyde (PFA) solution with picric acid (4% PFA, 0.4% picric acid in 0.16 M phosphate buffer solution (PBS), pH 7.4). The rat spinal cords were harvested to be fixed in 4% PFA for 3 days and preserved in 70% ethanol at 4 °C. The specimens were processed for contrast-enhanced μCT and routine histological evaluations. *Ex vivo* μCT evaluations were performed using high resolution μCT scanner (Skyscan 1076, Skyscan Kontich, Belgium), to visualise the three-dimensional morphology of rat spinal cord after soaking it in a hydrophilic iodinated contrast agent (Omipaque, GE Healthcare Ireland, Cork, Ireland, UK) in a 1:1 dilution with 1% PBS. The applied X-ray voltage was 100 kV with the filter as 1. Continuous scans were taken perpendicular to the longitudinal axis of the rat spinal cord with the isotropic voxel size being 9.0 μm. The intensities of the contrast medium in grey matter on the injured and non-injured sides were calculated to indicate tissue organisation.

2.6. Histological evaluations

After μCT scanning, the specimens were processed and embedded in paraffin. They were continuously sectioned by microtome with a thickness of 8 μm. The sections were stained by haematoxylin–eosin (H&E) and luxol fast blue (LFB), and then analysed under a microscopic imaging system (Leica Q500MC, Leica Cambridge

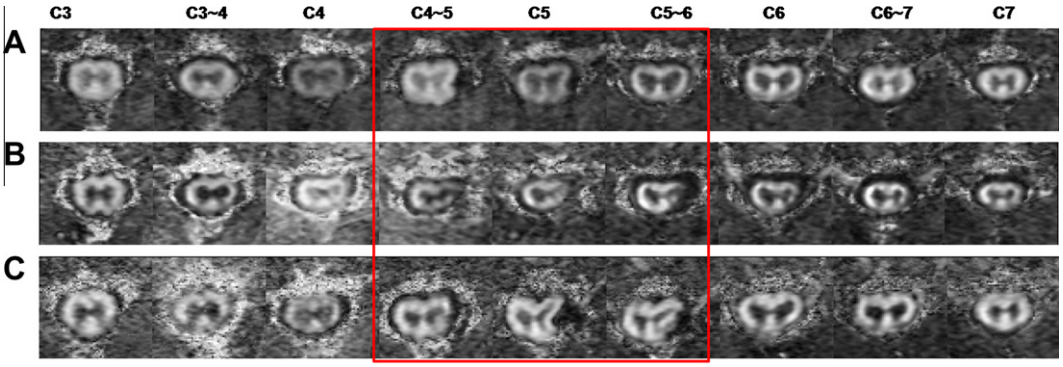

Fig. 3. The representative images showing the maps of fractional anisotropy (FA), generated from Diffusion Tensor Imaging (DTI) studio, along the spinal cord from caudal to rostral with increment of 2.2 mm in slice thickness in different group of model rats by SEP responses categorised by the amplitude and the latency (A, B and C). The lesions were localised on the postero–lateral sides at the level of C3–7of the cord (in red box).

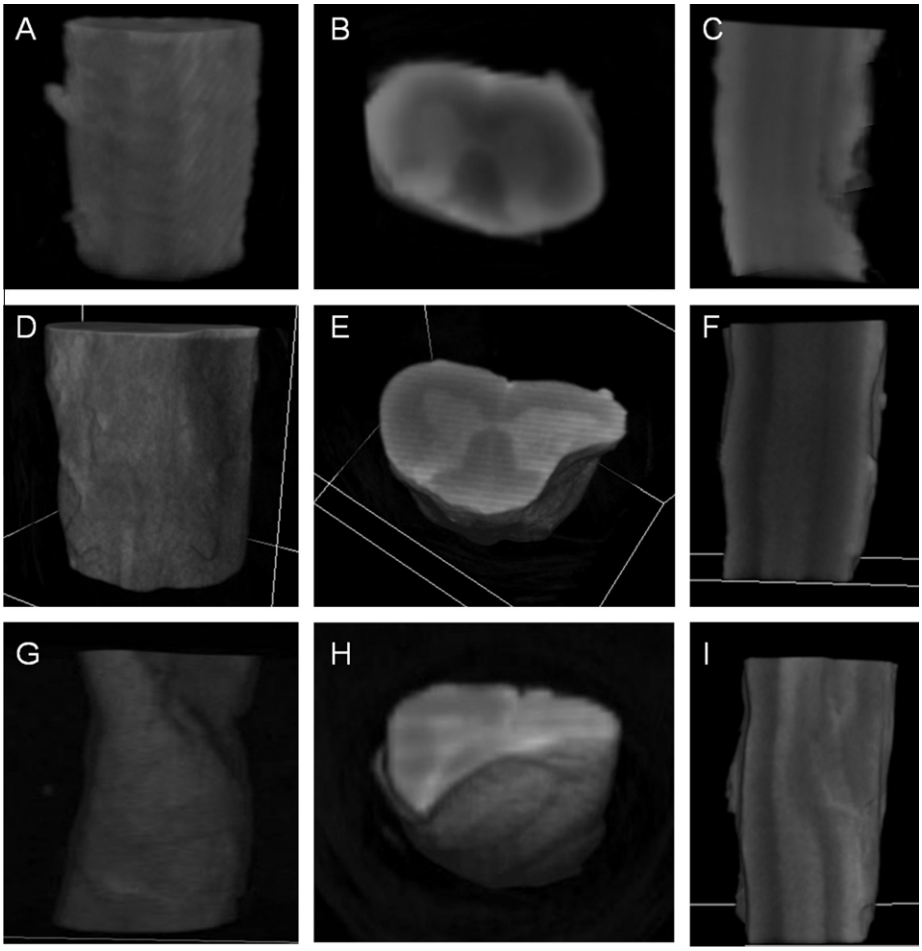

Fig. 4. The representative micro-CT images showing the gross morphology of the cord in model rats with different types of SEP response (type A: A–C; type B: D–F; type C: G–I). As compared with the model rats with either type A or B, it was noted that there existed significant deformity of the cord both white and gray matter in the model rats with type C.

Ltd., Cambridge, UK). LFB was employed to stain the myelin in white matter of the spinal cord and the blue colour intensity indicated the content of myelin. All neurons having clearly delineated centrally located nuclei and abundant Nissl bodies within the perikarya were identified following the method of Baba et al. (1996), and were counted on the injured and non-injured sides of grey matter among all model rats using Image J (National Institutes of Health, USA).

2.7. Statistical analysis

The comparisons for the ultrastructure of cord between on the injured and non-injured sides were performed using the paired *t*-test. The comparisons for the ultrastructural characteristics of spinal cords among the animals categorised by SEP responses were performed using one-way analysis of variance (ANOVA) and *post hoc* test. The level of significance was set at $p < 0.05$. All data anal-

Table 1
Functional and ultrastructural changes of rat spinal cord after chronic compression.

	Sides	SEP response		DTI	Micro-CT	Histology	
		Latency (ms)	Amplitude ($\times 10^{-3}$ mV)	FA – WM (0–1)	GM – contrast intensity (0–255)	Nr. of neurons (/mm^2)	LFB colour intensity (0–255)
Type A (n = 6)	N	15 ± 3	17 ± 3	0.73 ± 0.05	79 ± 7	29 ± 6	125 ± 8
	I	16 ± 2	14 ± 4	0.66 ± 0.04*	85 ± 6	24 ± 7	116 ± 7*
Type B (n = 5)	N	14 ± 3	15 ± 3*	0.68 ± 0.04$^{\#}$	84 ± 7	29 ± 7	119 ± 7$^{\#}$
	I	16 ± 3	7 ± 3$^{*,\#}$	0.61 ± 0.06$^{*,\#}$	88 ± 5	22 ± 8	108 ± 8$^{*,\#}$
Type C (n = 4)	N	17 ± 3	12 ± 4	0.67 ± 0.04$^{\#}$	80 ± 9	29 ± 7	112 ± 8$^{\#}$
	I	22 ± 4$^{*,\#}$	6 ± 2$^{*,\#}$	0.60 ± 0.05$^{*,\#}$	95 ± 10$^{*,\#}$	15 ± 6$^{*,\#}$	103 ± 7$^{*,\#}$

Note: I: injured side; N: non-injured side. FA: fractional anisotropy; WM: white matter; GM: gray matter.
* Indicated statistical significance ($p < 0.05$) in the difference between the compression ipsilateral and contralateral sides using paired t test.
$^{\#}$ Indicated statistical significance ($p < 0.05$) in the difference between various types of SEP responses using one-way ANOVA and *post hoc* test.

yses were performed using SPSS 15.0 analysis software (SPSS Inc., Chicago, IL, USA).

3. Results

As shown in Fig. 1, the compression was placed at the postero–lateral side of the cord at C5–6 region in model rats. At postoperative 6 months, the cord compression was confirmed under MRI and μCT evaluations among all 15 model rats (Figs. 3 and 4). The adjacent level above or below C5–6 was also affected by the compression. Among them, six model rats (40%, group A) showed the unchanged SEP responses on the injured side, and the remaining nine of them (60%) showed abnormal SEP responses including the decreased amplitude only (n = 5, group B) and the delayed latency (n = 4, group C) (Table 1). In all model rats, the insults of the cord circulation were shown under histological evaluations, including central canal enlargement, intra-tissue bleeding and increased blood vessels in the grey matter (Fig. 5).

In group A, the ultrastructural damage was detected in white matter on the injured side, which were indicated by lower fractional anisotropy (FA) and less luxol fast blue stain (Table 1). Histologically, the vacuolation changes were noted in grey matter on the injured side (Fig. 5).

In groups B and C, the ultrastructural damage of the cord was more pronounced and had gross appearance distortion (Figs. 3–6). It was detected under MRI and μCT evaluations that there existed significantly lower FA values and higher contrast medium intensity on the injured sides (Figs. 3 and 4). It was echoed by less myelin stain and more vacuoles in white and grey matters, respectively (Figs. 5 and 6). In addition, the FA values and the myelin stain in the white matter of group B and C were also significantly lower than those of the model rats of group A (Table 1). In group C, the number of neurons was significantly lower on the injured side than on the non-injured side. The neurons in grey matter were also significantly fewer that those of either group A or B (Fig. 5, Table 1).

4. Discussion

This study first uncovered the ultrastructural changes behind SEP responses to chronic compressive injure of the spinal cord in a rat model. The model rats with changed SEP responses showed more severe ultrastructural changes in the spinal cord with both grey and white matter involved. In the model rats with only SEP amplitude changes, the main pathological features were axon damage and demyelination in white matter, which were indicated by lower FA values under MR diffusion imaging and less luxol fast blue stain histologically (DeBoy et al., 2007). In the model rats with prolongation of latency, loss of motoneurons in the grey matter was found as well as damage to the white matter. These findings generated from this study suggested that the categorised SEP responses by the amplitude and latency were associated with the extent of the ultrastructural changes of the chronic compressive spinal cord. SEP might have good potential as an objective evaluation tool aiding in the diagnosis and prognostication of CSM clinically. It might also help to explain the phenomena reported in our previous clinical studies (Cheung et al., 2008; Hu et al., 2008). It was reported that the CSM patients with delayed latency had poor postoperative recovery ratio. It might be due to the irreversible loss of motoneurons in chronic compressive spinal cord. The patients who had unchanged SEP or the pure decreased amplitude had better outcome, which might be the result of the reversibility of ischaemia-related white matter damage.

SEP has been widely used as an intra-operative monitoring method in thoracic, cardiovascular and spinal surgery to detect

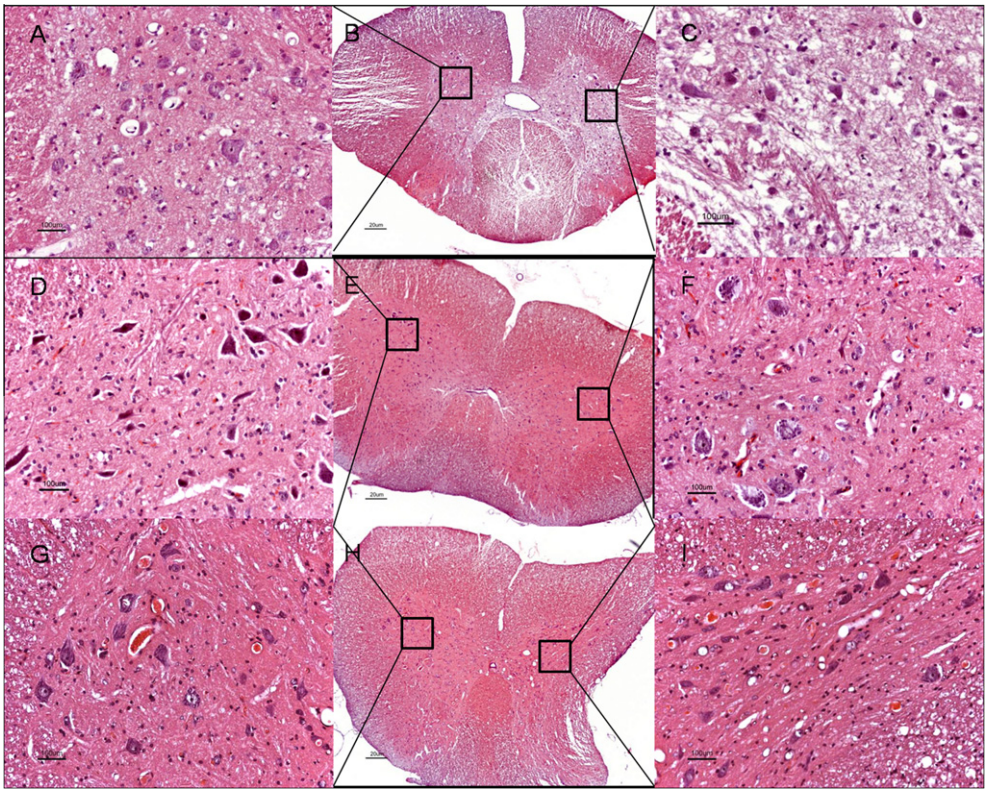

Fig. 5. The representative images showing the histological changes of the chronic compressed spinal cord in three groups of model rats with different SEP responses (Group a: A–C, Group B: D–F, and Group C: G–I). The circulation insult of the cord was noted among all model rats including central canal enlargement (B), intra-tissue bleeding (D–F) and increased blood vessels (G–I). The grey matter damages on the ipsilateral side of the compression (C, F and I) were more severe than the contralateral side (A, D and G) in all three groups. In group C, the gross appearance of the cord was significantly distorted and the number of neurons decreased with shrinkage (I). (Magnification B, E and H 4×; A, C, D, F, G, I: 20×; Haematoxylin and Eosin staining).

the acute spinal cord injuries, that is, mechanical traction, ischaemia, etc. (Seyal and Mull, 2002; Cruccu et al., 2008). Recently, the values of SEP in the diagnosis and prognostication of chronic spinal cord injuries have also been explored (Hu et al., 2008). In acute spinal cord injuries, the false-negative outcomes of SEP were rare (0.063%) (Seyal and Mull, 2002). However, there were 24–49% of CSM patients showing unchanged SEP responses as reported by us and others in previous clinical studies (Bednarik et al., 1999; Hu et al., 2008). In our rat model with the induced chronic compressive injuries of the spinal cord, there were 40% model rats who did not show any changes of SEP responses on the injured sides although there existed circulation insult. It suggested that the SEP might not be sensitive to chronic changes of the spinal cord and it may not be an alarming test for CSM, although its prognostic values have been strongly supported by our previous clinical and present experimental studies. It should be pointed out that the sensitivity of SEP for acute intra-operative injury is close to 100% and the earliest and reliable changes are seen in the amplitude instead of latency (Cheung et al., 2008; Hu et al., 2008). By contrast, the sensitivity of SEP for chronic compressive injury of the spinal cord was low and the latency appears to be a reliable parameter in indicating the irreversible ultrastructural damage of the spinal cord.

The insidious onset, the variety of the symptoms and signs and uncertainty of the pathophysiology of CSM pose a big challenge for orthopaedic surgeons in early diagnosis and precise prognostication (Baron and Young, 2007). An appropriate model was essential for better understanding of the CSM pathophysiology. The putative mechanism of CSM is static and dynamic mechanical compression along with secondary ischaemia of the spinal cord (Harkey and Al-Mefty, 1998; Baptiste and Fehlings, 2006; Baron and Young, 2007). In the past few years, various attempts have been carried out to induce a chronic compressive injury to the spinal cord with clipping, placement of wire and screw or transplantation of tumour cells (al-Mefty et al., 1993; Iwamoto et al., 1995; Izumida, 1995; Bruce et al., 2002; Hama and Sagen, 2007). Yet, the immediate damage and/or significant inflammatory reactions were induced. One of the key issues is the material which can be implanted into the epidural space to produce the desirable compression in a chronic course. Recently, a water-absorbing polyurethane elastomer was used in an attempt to produce the course of a compressive injury (Kim et al., 2004). However, it expanded to the maximum volume within 24 h after surgical implantation, and significant motor function deficit was reported within the first 2 weeks (Kim et al., 2004). In the present study, the authors modified the water-absorbing materials by encasing a sustained-release membrane to control the expansion rate to closely mimic the chronic course of CSM. Among all the 15 model rats, the mechanical compression and circulation compromise of the cord were confirmed under radiological and histological evaluations. The histological findings in our rat model, including the demyelination of white matter, the reduction in the number of neurons and cavitation changes of grey matter, were consistent with limited data from the autopsy specimens of CSM patients (Mair and Druckman, 1953; Ogino et al., 1983). It was also found that the rat spinal cord with a similar deformity after chronic compression showed different patterns of the functional and structural damage of the spinal cord parenchyma, that is, group A and B. It was compatible with previous clinical findings showing that the cord compression ratio appeared not to necessarily correlate with the severity of spinal cord damage (Matsumoto et al., 2000; Bednarik et al., 2004). A new finding from this study is that the extent of damage to functional integrity of the

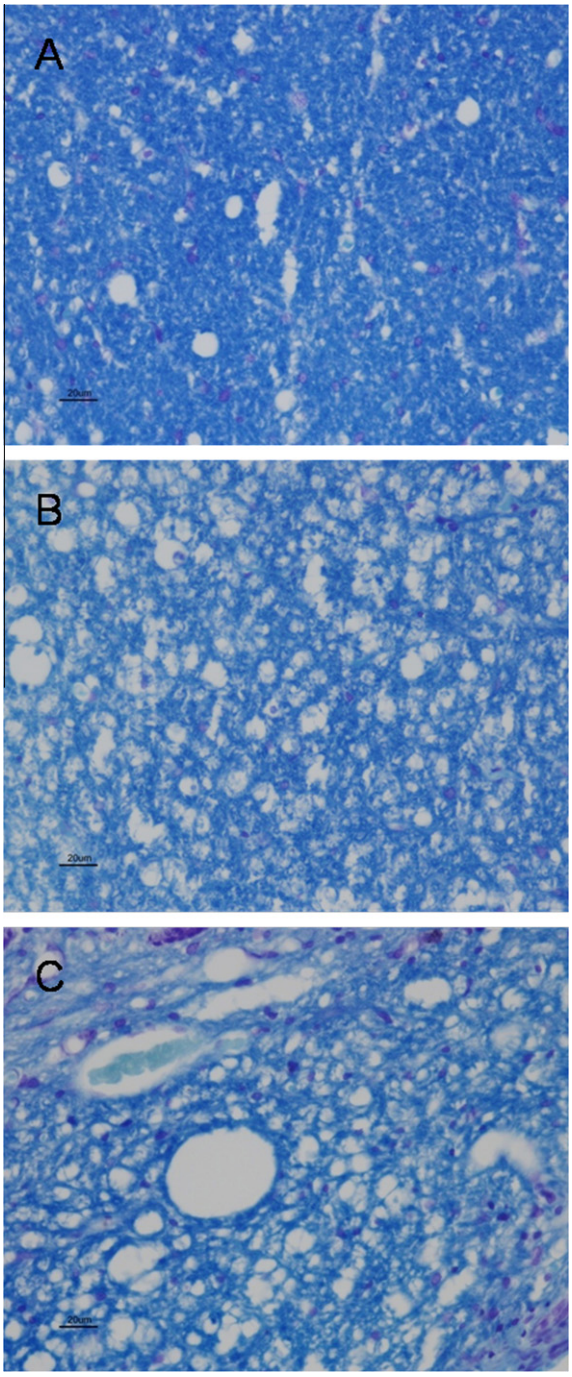

Fig. 6. The representative images showing the myelin staining in the white matter region of the chronic compressed spinal cords in three groups of model rats with different SEP responses (A–C). The less luxol fast blue stain and cavitation changes were noted in both group B and C in comparison with group A. (Magnification: 20×; luxol fast blue staining). (For interpretation of the references to colour in this figure legend, the reader is referred to the web version of this article.)

spinal cord, recorded by cortical SEPs, might be a good predictor for the extent of ultrastructural damage of chronically compressive spinal cord, which was verified by bioimaging and histological data.

Myelopathy might start when the cord becomes constricted in the canal. The vascular insufficiency was shown in the present study, that is, central canal enlargement and intra-tissue bleeding, which might be the result of occlusion of cerebral spinal fluid flow and venous congestion (Yoshizawa, 2002). It was known that oligodendrocytes play a crucial role in neurological development, protection, repair and damage, in particular for their role in formation and maintenance of myelin (Kim et al., 2003). They were particularly susceptible to ischaemia and underwent apoptosis with aggregation of the vascular insufficiency under chronic compression (Yamaura et al., 2002). It might account for the demyelisation and axon damage observed in our model with induced chronic compressive injury. Currently, there remains a debate as to whether CSM is caused mainly by direct compressive injuries due to narrowing of the canal or whether it is due to the compression-associated increased strain or shear or the compression-associated ischaemia of the enclosed cord (Baptiste and Fehlings, 2006). Our findings suggested that the circulation insult and demyelination changes of white matter might occur ahead of significant gross appearance changes of the cord. It might suggest that the protruded material in the canal initially interferes with the circulation of the enclosed cord leading to its demyelination changes and then causes gross appearance distortion gradually along with the loss of motoneurons. Therefore, the vascular event in the early phase of chronic compressive injures to the spinal cord should be paid attention to in future studies.

There are several limitations in the present study, including the following: (1) The study design of this study was only a cross-sectional observation to confirm the success of model establishment and characterise the pathophysiological changes in induced chronic compressive injuries of the cord. But the chronic course of spinal cord injuries and repair process should be further investigated. (2) The compression approach employed in the present study was through the lateral and dorsal aspects of the spinal cord. Actually in clinical scenario, the location of the offending pathology is ventral in cases with discs, spondylosis, OPLL, and it is dorsal in hypertrophied yellow ligament or both in developmental stenosis (Baron and Young, 2007). (3) The investigation of SEP responses in this study did not include peripheral nerve compound action potentials and subcortical recordings along the somatosensory pathway; actually, the additional spinal SEP recordings might be useful to clearly exclude possible peripheral nerve block of sensation; all these should be considered in the data interpretation in this study.

Acknowledgments

This work was partially supported by Hong Kong ITF Tier 3 (ITS/149/08), research Grants Council of the Hong Kong SAR, China (GRF771608M/GRF713006E) and the Seeding Funding Program of the University of Hong Kong. The authors would like to thanks Dr. Y. Guo and Dr. G. Zhao for surgical assistance in the establishment of the animal models.

References

al-Mefty O, Harkey HL, Marawi I, Haines DE, Peeler DF, Wilner HI, Smith RR, Holaday HR, Haining JL, Russell WF, et al. Experimental chronic compressive cervical myelopathy. J Neurosurg 1993;79:550–61.

Baba H, Maezawa Y, Imura S, Kawahara N, Nakahashi K, Tomita K. Quantitative analysis of the spinal cord motoneuron under chronic compression and experimental observation in the mouse. J Neurol 1996;243:109–16.

Baptiste DC, Fehlings MG. Pathophysiology of cervical myelopathy. Spine J 2006;6:190S–7S.

Baron EM, Young WF. Cervical spondylotic myelopathy: a brief review of its pathophysiology, clinical course, and diagnosis. Neurosurgery 2007;60:56–67.

Bednarik J, Kadanka Z, Dusek L, Novotny O, Surelova D, Urbanek I, Prokes B. Presymptomatic spondylotic cervical cord compression. Spine (Phila Pa 1976) 2004;29:2260–9.

Bednarik J, Kadanka Z, Vohanka S, Stejskal L, Vlach O, Schroder R. The value of somatosensory- and motor-evoked potentials in predicting and monitoring the effect of therapy in spondylotic cervical myelopathy. Prospective randomized study. Spine (Phila Pa 1976) 1999;24:1593–8.

Bouchard JA, Bohlman HH, Biro C. Intraoperative improvements of somatosensory evoked potentials: correlation to clinical outcome in surgery for cervical spondylitic myelopathy. Spine (Phila Pa 1976) 1996;21:589–94.

Bruce JC, Oatway MA, Weaver LC. Chronic pain after clip-compression injury of the rat spinal cord. Exp Neurol 2002;178:33–48.
Cheung MM, Li DT, Hui ES, Fan S, Ding AY, Hu Y, Wu EX. In vivo diffusion tensor imaging of chronic spinal cord compression in rat model. Conf Proc IEEE Eng Med Biol Soc 2009;1:2715–8.
Cheung WY, Arvinte D, Wong YW, Luk KD, Cheung KM. Neurological recovery after surgical decompression in patients with cervical spondylotic myelopathy – A prospective study. Int Orthop 2008;32:273–8.
Cruccu G, Aminoff MJ, Curio G, Guerit JM, Kakigi R, Mauguiere F, Rossini PM, Treede RD, Garcia-Larrea L. Recommendations for the clinical use of somatosensory-evoked potentials. Clin Neurophysiol 2008;119:1705–19.
DeBoy CA, Zhang J, Dike S, Shats I, Jones M, Reich DS, Mori S, Nguyen T, Rothstein B, Miller RH, Griffin JT, Kerr DA, Calabresi PA. High resolution diffusion tensor imaging of axonal damage in focal inflammatory and demyelinating lesions in rat spinal cord. Brain 2007;130:2199–210.
Hama A, Sagen J. Behavioral characterization and effect of clinical drugs in a rat model of pain following spinal cord compression. Brain Res 2007;1185:117–28.
Harkey HL, Al-Mefty O. The Pathophysiology of Chronic Compressive Cervical Myelopathy. In: Ono K, editor. Cervical Spondylosis and Similar Disorders. Singapore: World Scientific Publishing Co. Pvt. Ltd.; 1998. pp. 141–166.
Hu Y, Ding Y, Ruan D, Wong YW, Cheung KM, Luk KD. Prognostic value of somatosensory-evoked potentials in the surgical management of cervical spondylotic myelopathy. Spine (Phila Pa 1976) 2008;33:E305–10.
Hu Y, Luk KD, Lu WW, Leong JC. Application of time–frequency analysis to somatosensory evoked potential for intraoperative spinal cord monitoring. J Neurol Neurosurg Psychiatry 2003;74:82–7.
Ichihara K, Taguchi T, Sakuramoto I, Kawano S, Kawai S. Mechanism of the spinal cord injury and the cervical spondylotic myelopathy: new approach based on the mechanical features of the spinal cord white and gray matter. J Neurosurg 2003;99:278–85.
Iwamoto H, Kuwahara H, Matsuda H, Noriage A, Yamano Y. Production of chronic compression of the cauda equina in rats for use in studies of lumbar spinal canal stenosis. Spine (Phila Pa 1976) 1995;20:2750–7.
Izumida M. A chronic spinal cord compression model in a rat with a 354A tumor. Nippon Seikeigeka Gakkai Zasshi 1995;69:977–91.
Kim DH, Vaccaro AR, Henderson FC, Benzel EC. Molecular biology of cervical myelopathy and spinal cord injury: role of oligodendrocyte apoptosis. Spine J 2003;3:510–9.
Kim P, Haisa T, Kawamoto T, Kirino T, Wakai S. Delayed Myelopathy Induced by Chronic Compression in the Rat Spinal Cord. Ann Neurol 2004;55:503–11.
Lo YL. The role of electrophysiology in the diagnosis and management of cervical spondylotic myelopathy. Ann Acad Med Singapore 2007;36:886–93.
Lo YL. How has electrophysiology changed the management of cervical spondylotic myelopathy? Eur J Neurol 2008;15:781–6.
Mair WG, Druckman R. The pathology of spinal cord lesions and their relation to the clinical features in protrusion of cervical intervertebral discs; a report of four cases. Brain 1953;76:70–91.
Matsumoto M, Toyama Y, Ishikawa M, Chiba K, Suzuki N, Fujimura Y. Increased signal intensity of the spinal cord on magnetic resonance images in cervical compressive myelopathy. Does it predict the outcome of conservative treatment? Spine (Phila Pa 1976) 2000;25:677–82.
McCormick WE, Steinmetz MP, Benzel EC. Cervical spondylotic myelopathy: make the difficult diagnosis, then refer for surgery. Cleve Clin J Med 2003;70:899–904.
Morishita Y, Hida S, Naito M, Matsushima U. Evaluation of cervical spondylotic myelopathy using somatosensory-evoked potentials. Int Orthop 2005;29:343–6.
Ogino H, Tada K, Okada K, Yonenobu K, Yamamoto T, Ono K, Namiki H. Canal diameter, anteroposterior compression ratio, and spondylotic myelopathy of the cervical spine. Spine (Phila Pa 1976) 1983;8:1–15.
Rao R. Neck Pain, Cervical Radiculopathy, and Cervical Myelopathy: Pathophysiology, Natural History, and Clinical Evaluation. J Bone Joint Surg Am 2002;84:1872–81.
Robinson LR, Micklesen PJ, Tirschwell DL, Lew HL. Predictive value of somatosensory evoked potentials for awakening from coma. Crit Care Med 2003;31:960–7.
Seyal M, Mull B. Mechanisms of signal change during intraoperative somatosensory evoked potential monitoring of the spinal cord. J Clin Neurophysiol 2002;19:409–15.
Yamaura I, Yone K, Nakahara S, Nagamine T, Baba H, Uchida K, Komiya S. Mechanism of destructive pathologic changes in the spinal cord under chronic mechanical compression. Spine (Phila Pa 1976) 2002;27:21–6.
Yoshizawa H. Presidential address: pathomechanism of myelopathy and radiculopathy from the viewpoint of blood flow and cerebrospinal fluid flow including a short historical review. Spine (Phila Pa 1976) 2002;27:1255–1263.
Zhang ZG, Yang JL, Chan SC, Luk KD, Hu Y. Time-frequency component analysis of somatosensory evoked potentials in rats. Biomed Eng Online 2009;8:4.